

Heteroclinic bifurcations and chaotic transport in the two-harmonic standard map

Héctor E. Lomelí

Department of Mathematics, Instituto Tecnológico Autónomo de México ITAM, Río Hondo #1, México DF 01000

Renato Calleja

Department of Mathematics, University of Texas at Austin, Austin, Texas 78712

(Received 4 August 2005; accepted 31 January 2006; published online 31 May 2006)

We study a two-parameter family of standard maps: the so-called two-harmonic family. In particular, we study the areas of lobes formed by the stable and unstable manifolds. Variational methods are used to find heteroclinic orbits and their action. A specific pair of heteroclinic orbits is used to define a difference in action function and to study bifurcations in the stable and unstable manifolds. Using this idea, two phenomena are studied: the change of orientation of lobes and tangential intersections of stable and unstable manifolds. © 2006 American Institute of Physics.

[DOI: 10.1063/1.2179647]

The standard family of maps, or Chirikov model, is a discrete time dynamical system that has been studied by many authors. Its importance is due to the fact that it has many of the dynamic properties of Hamiltonian systems. In many situations, as one varies the parameters of the family many interesting bifurcations appear. We study a variation of the classic standard map in which, adding an extra term, we get the so-called two-harmonic model. In particular, we study heteroclinic orbits and the phenomenon of chaotic transport.

I. INTRODUCTION

Standard maps are area-preserving diffeomorphisms of \mathbb{R}^2 given by

$$(\theta', r') = f(\theta, r) = (\theta + r + V'(\theta), r + V'(\theta)), \quad (1)$$

where V is called the potential and, in most cases, is a periodic function. In particular, the two-harmonic map is a member of the standard map family, with potential given by

$$V_{a,b}(\theta) = -\frac{a}{2\pi} \cos(2\pi\theta) - \frac{b}{4\pi} \cos(4\pi\theta), \quad (2)$$

and therefore,

$$\theta' = \theta + r + a \sin(2\pi\theta) + b \sin(4\pi\theta), \quad (3)$$

$$r' = r + a \sin(2\pi\theta) + b \sin(4\pi\theta). \quad (4)$$

As far as we know, the two-harmonic map was first studied by Baesens and Mackay in Ref. 2. They were interested in studying *cantori* for different values of the parameter space. In this paper, we analyze another set of dynamically relevant invariants: the stable and unstable manifolds of fixed points and their heteroclinic intersections. We have found some interesting phenomena related to chaotic transport.

Some standard maps have a useful property. If the potential V is an odd function, then they possess a discrete

symmetry that allows us to simplify the search of heteroclinic connections. This special type of symmetry is called a *reversor* and consists of a map $R: \mathbb{R}^2 \rightarrow \mathbb{R}^2$ such that R is an involution (i.e. $R^2 = id$) and $R \circ f = f^{-1} \circ R$. In Ref. 7, this idea was used to find heteroclinic connections in a perturbed integrable map. Notice that, if R is a reversor, so is $f \circ R$.

Let V be a potential function such that $V(-\theta) = V(\theta)$. Then, $V'(-\theta) = -V'(\theta)$ and $R(\theta, r) = (-\theta, r + V'(\theta))$ is a reversor for the standard map [(3) and (4)]. Let $\text{Fix}\{R\}$ be the set of fixed points of the reversor. It is clear that if p^* is a fixed point then Rp^* is also a fixed point and

$$\begin{aligned} \text{Fix}\{R\} \cap W^s(p^*) \\ = \text{Fix}\{R\} \cap W^u(Rp^*) \subset W^s(p^*) \cap W^u(Rp^*). \end{aligned}$$

In this way, each point in $\text{Fix}\{R\} \cap W^s(p^*)$ is heteroclinic. If we use a secant-like argument to search for points in $\text{Fix}\{R\} \cap W^s(p^*)$, we can find heteroclinic orbits that cross the set $\text{Fix}\{R\}$. In the same way, we find heteroclinic orbits that intersect the fixed set $\text{Fix}\{f \circ R\}$ of the reversor $f \circ R$.

It is a well known fact that heteroclinic orbits have an invariant called *action*. In our example, it turns out that, for most parameters (a, b) , the actions of these orbits are different. Using the pair of heteroclinic orbits that arise from the reversor method, we can systematically study the difference in action between them.

The difference in action function is formally introduced in Sec. III and will be denoted as $\Lambda(a, b)$ in the case of the dynamics corresponding to the parameters (a, b) . In some cases, the choice of parameters (a, b) will give a value of $\Lambda(a, b)$ that corresponds to the area of a lobe. We have found that the function $\Lambda(a, b)$ can change sign, a situation that appears when the dynamic properties of the two heteroclinic orbits suffer a bifurcation. In addition, the function Λ can have discontinuities. In this paper we try to explain these two situations, and relate them with dynamic relevant behavior.

A simple approximation of the difference in action function $\Lambda(a, b)$ of the two-harmonic standard map, can lead us to discover a dynamic behavior that the usual standard map or Chirikov map apparently does not have. We will argue that some values of the parameters for which the action difference vanishes are linked to integrability. For these values, the stable manifold of a hyperbolic fixed point seems to approach a segment of the unstable manifold of an adjacent fixed point bounded by $\text{Fix}\{R\}$ and $\text{Fix}\{fR\}$.

The splitting of separatrices is closely related to chaotic behavior of the system, and a common way to measure this splitting is by measuring the angle of intersection of the stable and unstable manifolds at $\text{Fix}\{R\}$ (see Refs. 5 and 21). In our case, as the transverse intersections change orientation, there is a point where the angle appears to vanish.

The difference in action function Λ proved to be useful for other purposes. The existence of tangent intersections on the separatrices is detected from the analysis of discontinuities of the function $\Lambda(a, b)$. These intersections explain the sudden changes in the position of points of the heteroclinic orbits that are used to approximate this function. In our system, tangential behavior is produced by the influence of a $1/2$ -periodic term of the potential in the generating function. Thus, the standard map cannot have this sort of intersections near the sets $\text{Fix}\{R\}$ and $\text{Fix}\{fR\}$.

Numerical computations show that this intersections become more frequent as the parameter a is closer to zero. Intuitively, we may think that as we take the limit with a goes to zero we should find a situation close to a “twin separatrix”-like picture; i.e., the phase space is twice the usual standard map phase space, one next to the other with half the original size. As the b grows away from zero, lobes start intersecting tangentially from really small values of the parameter. We can imagine that intersections will be more and more common for smaller values of b . Our method is able to detect this situation.

The two-harmonic map is a simple example of a standard type map that shows dynamical properties that may be of interest. The two different types of bifurcations presented in this paper have distinct natures and, therefore, can be used for different research purposes.

II. COMPUTATION OF HETEROCLINIC ORBITS

Let $T = \mathbb{R}/\mathbb{Z}$ be the circle. Standard maps are exact symplectic diffeomorphisms of the annulus $A = T^*(T) = T \times \mathbb{R}$ given, in (θ, r) coordinates, by (1). The case wherein $V(\theta) = (k/4\pi^2)\cos(2\pi\theta)$ is known as the standard map or Chirikov model.

Consider the standard lift $\kappa : \mathbb{R}^2 \rightarrow A$. If $\tilde{F} : A \rightarrow A$ is a C^1 function of the annulus, we can lift it to a C^1 function of \mathbb{R}^2 that commutes with κ as follows: $\tilde{F} \circ \kappa = \kappa \circ F$. Let $\tilde{\lambda}$ be Liouville one-form for A and $\lambda = \kappa^* \tilde{\lambda}$ the corresponding one-form on the cover. In (θ, r) coordinates, λ can be written as $\lambda = rd\theta$.

Definition 1. A C^1 diffeomorphism \tilde{F} of the annulus A is called a twist map if

- a) \tilde{F} is homotopic to the identity,

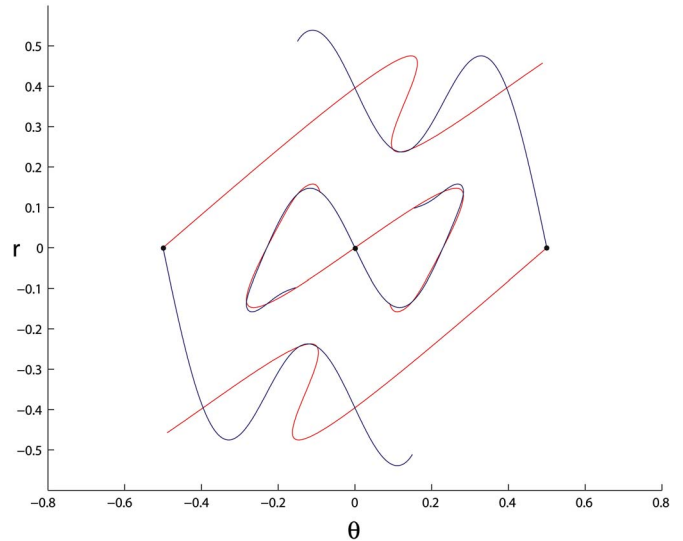


FIG. 1. Stable and unstable manifolds in the two-harmonic map phase space, $a = -0.1910$ and $b = 0.2$. The origin is hyperbolic and has no heteroclinic connections with p_1 or p_2 .

- b) the one-form $\tilde{F}^* \tilde{\lambda} - \tilde{\lambda}$ is exact,
- c) if $(\theta', r') = F(\theta, r)$ is a lift of \tilde{F} , then $\psi(\theta, r) = (\theta, \theta')$ is a diffeomorphism.

The second and third conditions of the definition above imply^{6,10} that a twist map has a Lagrangian generating function $S(\theta, \theta')$, which generates the map implicitly through the equations $r = -\partial_1 S(\theta, \theta')$ and $r' = \partial_2 S(\theta, \theta')$. Thus, to generate a map, S must satisfy the *twist condition* that the second equation above can be inverted to obtain $\theta'(r, \theta)$. This occurs, for instance, if $\partial_1 \partial_2 S < 0$, and implies the geometric condition that vertical lines tilt to the right upon iteration: $\partial \theta' / \partial r > 0$. Furthermore, we assume that our twist map has *zero net flux*, which is equivalent to $S(\theta + k, \theta' + k) = S(\theta, \theta')$, for all $k \in \mathbb{Z}$.

Let $\tilde{f} : T \times \mathbb{R} \rightarrow T \times \mathbb{R}$ be a standard map with lift $f : \mathbb{R}^2 \rightarrow \mathbb{R}^2$ and generating function

$$S(\theta, \theta') = \frac{1}{2}(\theta - \theta')^2 + V_{a,b}(\theta). \tag{5}$$

We assume that the potential $V_{a,b}(\theta)$ is given by expression (2).

This standard-like map is called the two-harmonic map and has been studied by Baesens and MacKay in Ref. 2. When $b = 0$ and $a = \varepsilon / (2\pi)$, the potential (2) generates the Chirikov model. Therefore, the two-harmonic map includes the dynamics of the Chirikov model and adds a $1/2$ -periodic perturbation.

In the main phase space of f , we find two hyperbolic fixed points at $p_1 = (-1/2, 0)$ and $p_2 = (1/2, 0)$, which are connected with heteroclinic orbits that correspond to the intersections of the stable and unstable manifolds. There is also a fixed point at the origin. This point is elliptic for $b = 0$ and, as we move b away from zero, its stability changes and becomes hyperbolic. We notice that, as the elliptic fixed point turns hyperbolic, homoclinic orbits appear (see Fig. 1).

We also notice that for some choices of parameters, heteroclinic orbits between the origin and p_1 and p_2 emerge. For

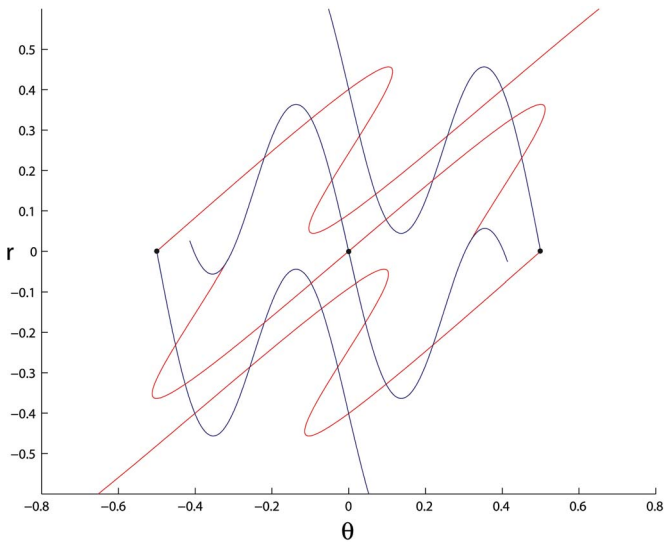


FIG. 2. Stable and unstable manifolds in the two-harmonic map phase space, $a=-0.057$ and $b=0.3$. The origin is hyperbolic and has heteroclinic connections with p_1 and p_2 .

instance, the case of $a=-0.057$ and $b=0.3$ is shown in Fig. 2. This can be explained by a result of Wang that can be found in Refs. 18 and 19. The result assures the existence of heteroclinic orbits between the origin and p_2 (and between the origin and p_1), given that there is a separating barrier in the potential between the two points.

In his work,^{12,18,19} Wang proves the following. Let $\varphi(\theta)=S(\theta, \theta)$ be a C^2 function with two local minima θ^1 and θ^2 such that $\varphi(\theta^1)=\varphi(\theta^2)<\varphi(x)$ for all $x \in (\theta^1, \theta^2)$. Then there exist heteroclinic connections between θ^1 and θ^2 .

A similar result was proved by Tabacman.¹⁷ For his proof, Tabacman uses a different method also based in variational principles and the next result.

Proposition 1. *Let $p_1=(\theta^1, r^1)$ and $p_2=(\theta^2, r^2)$ be two hyperbolic fixed points for a symplectic twist map f . Let U_1 and U_2 be neighborhoods of θ^1 and θ^2 on which the graph of the derivative of the functions Φ^u and Φ^s , respectively, give the unstable manifold of p_1 and the stable manifold of p_2 . Then the critical points of the function*

$$W(\theta_0, \dots, \theta_N) = \Phi^u(\theta_0) + \sum_{k=0}^{N-1} S(\theta_k, \theta_{k+1}) - \Phi^s(\theta_N),$$

where $\theta_0 \in U_1$ and $\theta_N \in U_2$, are segments of heteroclinic orbits.

From this, a numerical algorithm emerges. Golé⁴ summarizes it in five steps:

- Find the fixed points to connect p_1, p_2 . Find approximations of the unstable manifold of p_1 .
- Compute an approximation to Φ^u by using an approximation of the stable manifold.
- Perform similar steps to approximate Φ^s at p_2 .
- Pick N (large enough) and use your favorite numerical method to compute critical points of the function W defined above, with points θ_0 and θ_N suitably close to p_1 and p_2 , respectively.

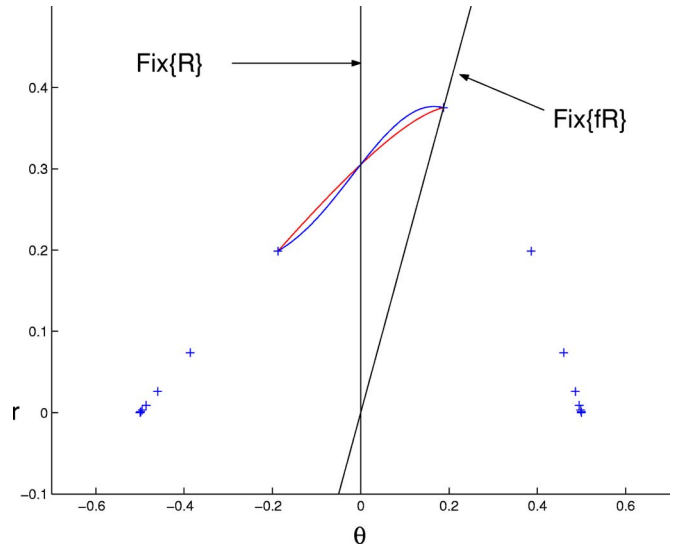


FIG. 3. Turnstiles near $\text{Fix}\{R\}$ and $\text{Fix}\{fR\}$ for $a=-0.1910, b=0$. The plus signs (+) represent the minimizing heteroclinic orbit that intersects $\text{Fix}\{fR\}$.

- For more precision, make θ_0 and θ_N closer to p_1 and p_2 , respectively, and increase the number N .

We have used this algorithm to find heteroclinic connections for our standard map using the “trust region” method described in Ref. 11 with $N=29$. An application of this algorithm to the two-harmonic map is presented in Figs. 3 and 4.

Increasing b away from zero, we discover that, after a while, the intersections in heteroclinic points change orientation. When such orientation changes, we can observe that the algorithm converges to a different orbit. Using the reversibility properties of the standard maps (discussed in Refs. 7 and 15) and the reversor

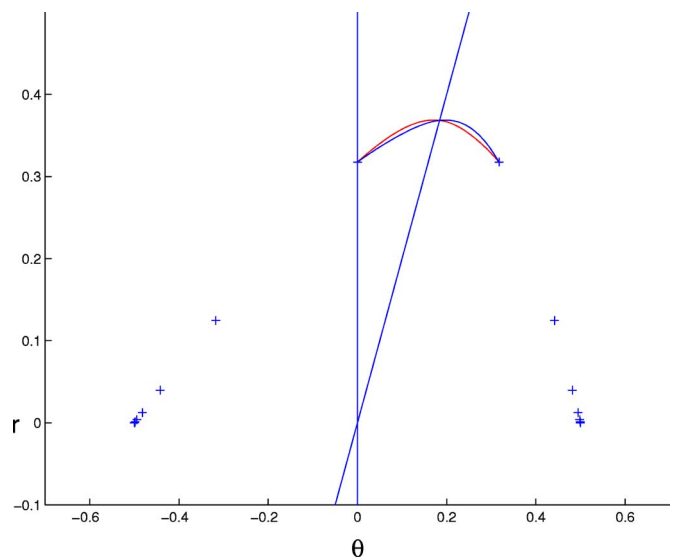


FIG. 4. Turnstiles near $\text{Fix}\{R\}$ and $\text{Fix}\{fR\}$ for $a=-0.1910, b=0.025$. The plus signs (+) represent the minimizing heteroclinic orbit that intersects $\text{Fix}\{R\}$.

$$R : (\theta, r) \rightarrow (-\theta, r + V'_{a,b}(\theta)), \tag{6}$$

we find that the new orbit is, indeed, heteroclinic. Since the method is designed to converge to minimizing orbits, we may suspect that a minimizing heteroclinic orbit turns into a max-min heteroclinic orbit as the orientation of the heteroclinic intersections change.

III. ACTION AND TRANSPORT

In the preceding section, we described a numerical example in which a change of orientation of the stable and unstable manifolds is observed. In this section, we try to explain what happens at the instant when this topological shift occurs. In order to do so, we will identify a connection between this topological property and the roots of the function Λ described in Sec. I as the “action difference function.” Moreover, we show a connection between the two-harmonic standard map and an integrable map known as the Suris map.⁷

A way of measuring transport is by approximating the first intersection of the sets $\text{Fix}\{R\}$ and $\text{Fix}\{fR\}$ with the invariant manifolds, $W^u(p_1)$ and $W^s(p_2)$, of two adjacent hyperbolic fixed points, as was mentioned in Sec. I. We denote these two points of intersection as q_0^R and q_0^{fR} , respectively. We then check that these two points belong to two neighboring heteroclinic orbits, and we evaluate the expression

$$A^u - A^s = \sum_{j=-\infty}^{\infty} (S(\theta_j^R, \theta_{j+1}^R) - S(\theta_j^{fR}, \theta_{j+1}^{fR})), \tag{7}$$

where θ_j^R and θ_j^{fR} are the first components of the j -th iterates of q_0^R and q_0^{fR} , respectively (see, for example, Ref. 8). Thus, the transport function is an action difference function of two disjoint adjacent heteroclinic orbits. [We use the $<_u$ order described in Ref. 20. Suppose that $q_1, q_2 \in W^u(p_i)$, then $q_1 <_u q_2$ if q_1 is closer to p_i than to q_2 in the sense of arc length along $W^u(p_i)$.]

Proposition 2. q_0^R and q_0^{fR} belong to two different heteroclinic orbits.

Proof. Suppose that for some integer n , we have that

$$f^n(q_0^R) \in \text{Fix}\{fR\}.$$

It follows, from the properties of the reversor R , that $f^{2n-1}(q_0^R) = q_0^R$. However, this is impossible, since $q_0^R \in W^u(p_1) \cap W^s(p_2)$. \square

Measuring transport of the two-harmonic map can be a more difficult task, since some pairs of parameters (a, b) allow heteroclinic points to exist between $q_0^R(a, b)$ and $q_0^{fR}(a, b)$. Therefore, instead of trying to measure the transport, we approximate the action difference of the orbits of $q_0^R(a, b)$ and $q_0^{fR}(a, b)$. For each $(\theta, r) \in \mathbb{R}^2$, let $\pi_1(\theta, r) = \theta$. We define a function that depends on the parameters of the two-harmonic map,

$$\Lambda(a, b) = \sum_{j=-\infty}^{\infty} \Delta S_j(a, b), \tag{8}$$

where

$$\Delta S_j(a, b) = S(w_j(a, b), w_{j+1}(a, b)) - S(z_j(a, b), z_{j+1}(a, b))$$

with

$$w_j(a, b) = \pi_1(q_j^R(a, b))$$

and

$$z_j(a, b) = \pi_1(q_j^{fR}(a, b)),$$

the first components of the two heteroclinic orbits.

As in Eq. (7), an important observation⁹ is that, when $q_0^R(a, b)$ and $q_0^{fR}(a, b)$ belong to two neighboring orbits, the absolute value $|\Lambda(a, b)|$ measures the transport across the separatrix formed by stable and unstable manifold segments. Otherwise, this equation measures the algebraic area bounded by

$$\mathcal{S}[q_0^R(a, b), q_0^{fR}(a, b)],$$

and

$$\mathcal{U}[q_0^R(a, b), q_0^{fR}(a, b)]$$

(see, for example, Ref. 10). The area of a lobe is positive whenever the unstable segment is over the stable segment and negative when the stable segment is above. As the intersection orientation changes, we expect to see a change of the lobe flux sign. If so, action difference is null where the orientation changes. [Here we use the notation of Ref. 20. Let $q_1, q_2 \in W^s(p_i) (\in W^u(p_i))$ such that $q_1 <_s q_2$ ($q_1 <_u q_2$), then $\mathcal{S}[q_1, q_2]$ ($\mathcal{U}[q_1, q_2]$) is the stable (unstable) segment between q_1 and q_2 .]

When measuring the amount of stochastic behavior of the Chirikov map, many attempts have proven successful. As it was said in Sec. I, a common method is to connect the measure of the splitting of the separatrix with the measure of the angle α of intersection of the stable and unstable manifolds at $\text{Fix}\{R\}$. In Ref. 5, Lazutkin gives an asymptotic formula for α in a standard map with potential $V(\theta) = (-\varepsilon/2\pi)\cos(2\pi\theta)$,

$$\alpha \sim C_1 \frac{e^{-\pi^2/\sqrt{\varepsilon}}}{\varepsilon}$$

as $\varepsilon \rightarrow 0$. Since the two-harmonic map turns into the Chirikov map when $b=0$, we can expect that, as $a \rightarrow 0$, the asymptotic relation

$$\Lambda(a, 0) \sim C \frac{e^{-\pi^2/\sqrt{|a|}}}{a}$$

holds for some constant C that is independent of a .

In our numerical explorations, we try to detect changes of the sign of the angle α for positive values of b . Thus, the method that we propose allows us to find changes in the intersections orientation using the set of roots of the action difference function (8). A previous classification of these annihilating values must be done since the function does not measure a geometric area but an algebraic one. It is possible to get a couple of parameters (a^*, b^*) such that $\Lambda(a^*, b^*) = 0$, while the angle α is not close to zero. We illustrate this pathological case with an example.

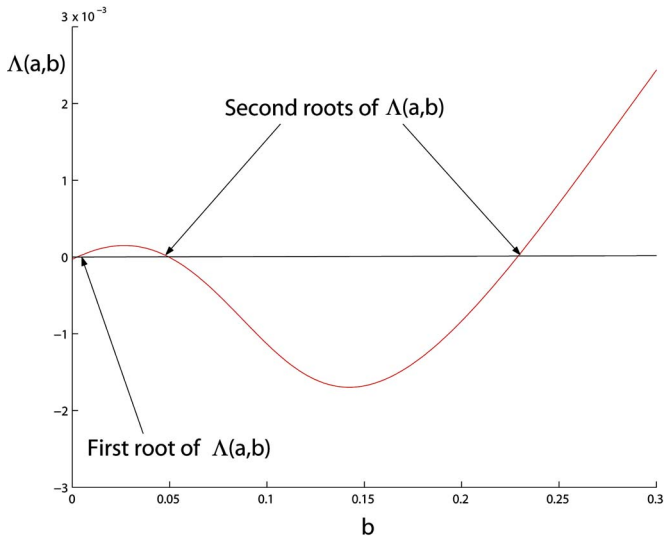


FIG. 5. $\Lambda(a,b)$ for $a=-0.1$.

In Fig. 5, we show the graph of the transport with fixed $a=-0.1$ and b between 0 and 0.3. Notice that the Λ has three roots for this single value of a . If we plot the invariant manifolds corresponding to these three roots, we discover that the first root, $b \approx 0.0043$, corresponds to a parameter where the angle of intersection of the stable and unstable manifolds tends to zero (see Fig. 6). The other two roots are not related with small angles. The total area $\Lambda(a,b)$ is null because a complete turnstile having two same sized lobes is trapped between $q_0^R(a,b)$ and $q_0^{fR}(a,b)$; i.e., the incoming flux is equal to the outgoing flux (see Fig. 7). Thus, we need to classify the roots of $\Lambda(a,b)$ in two groups. A pair of parameters (a,b) is called first root if the angle of intersection of the stable and unstable manifolds α changes sign in a neighborhood of (a,b) (see Figs. 8 and 9). The pair is called second root when the angle is far from zero (a,b) . Thus, a second root is a pair of parameters (a,b) where the action difference is annihilated by cancellation of lobe areas.

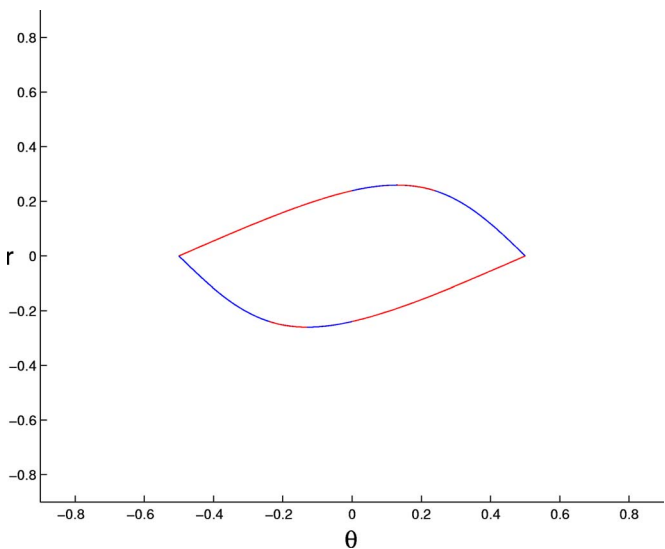


FIG. 6. For the pair of parameters $a=-0.1$ and $b \approx 0.0043$, the invariant manifolds between $q_0^R(a,b)$ and $q_0^{fR}(a,b)$.

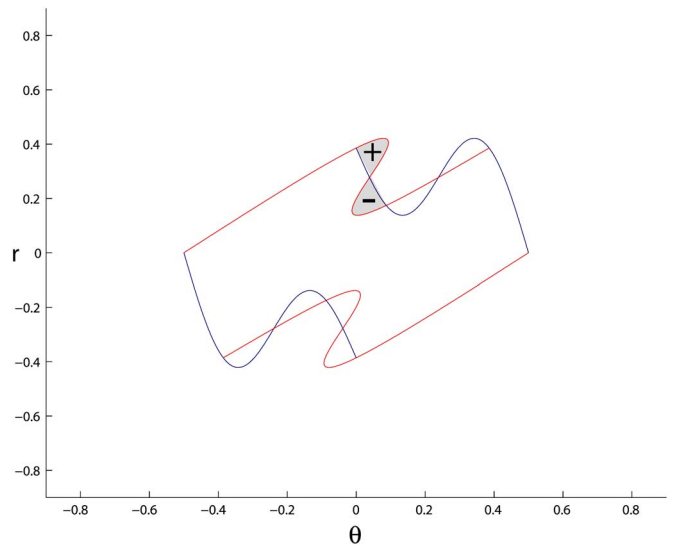


FIG. 7. For the pair of parameters $a=-0.1$ and $b \approx 0.225$, the function Λ vanishes, but the manifolds intersect transversally.

A possible explanation of the bifurcation that we just analyzed is based on the integrability of certain standard maps. The Suris map is a standard map generated by (5) with the potential

$$\tilde{V}_\delta(\theta) = -\frac{2}{\pi} \int_0^\theta \arctan\left(\frac{\delta \sin(2\pi t)}{1 + \delta \cos(2\pi t)}\right) dt. \tag{9}$$

Suris showed that this map is Liouville integrable¹⁶ for all δ . Its integral is given explicitly by the equation

$$I_\delta(\theta, r) = \cos(\pi r) + \delta \cos(\pi(2\theta - r)). \tag{10}$$

This map has been rediscovered by several authors. For example, in Ref. 3 an equivalent map, known as Hirota map, is used for the study of sine-Gordon models in light-like lattices.

We would like to explain the change of sign of the function Λ based on the integrability of the Suris map. In order to

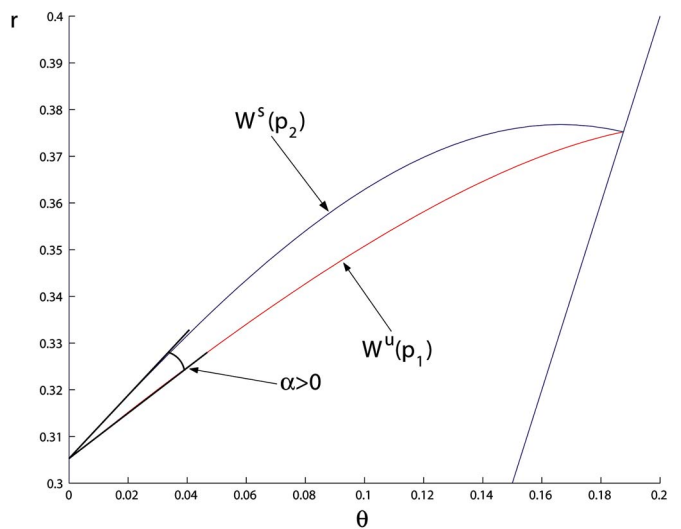


FIG. 8. Lobe trapped between $\text{Fix}\{R\}$ and $\text{Fix}\{fR\}$ for parameters $a = -0.1910$, $b=0$.

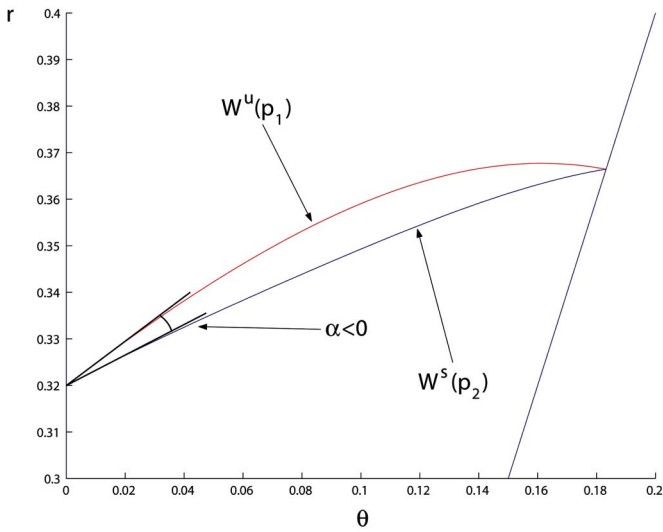


FIG. 9. Lobe trapped between $\text{Fix}\{R\}$ and $\text{Fix}\{fR\}$ for parameters $a=-0.1910, b=0.025$.

do this, we will relate the two-harmonic map and the Suris map via the Fourier coefficients of the function

$$\tilde{V}'_{\delta}(\theta) = -\frac{2}{\pi} \arctan\left(\frac{\delta \sin(2\pi\theta)}{1 + \delta \cos(2\pi\theta)}\right).$$

Since $\tilde{V}'_{\delta}(\theta)$ is an odd function, the even Fourier coefficients are zero. We compute the first two odd coefficients in the interval $[-1/2, 1/2]$:

$$d_1 = 2 \int_{-1/2}^{1/2} \tilde{V}'_{\delta}(\theta) \sin(2\pi\theta) d\theta = \frac{-2\delta}{\pi}$$

and

$$d_2 = 2 \int_{-1/2}^{1/2} \tilde{V}'_{\delta}(\theta) \sin(4\pi\theta) d\theta = \frac{\delta^2}{\pi}.$$

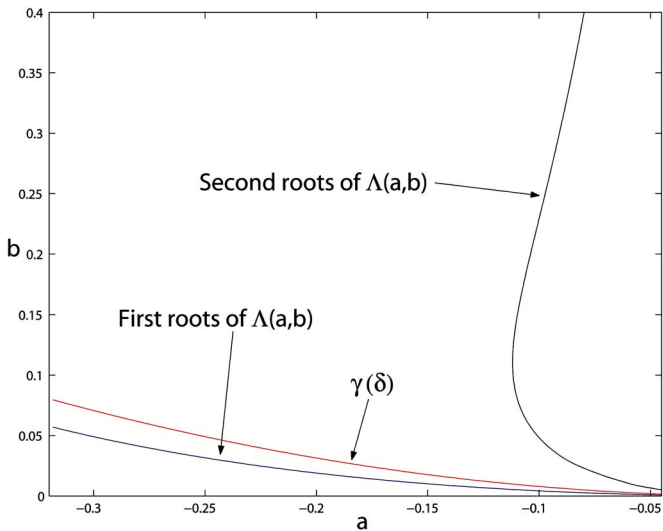


FIG. 10. Two-harmonic map parameter space.

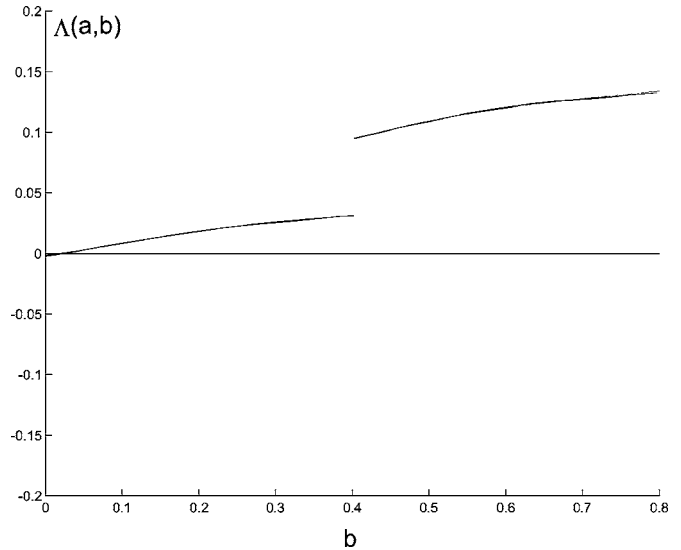


FIG. 11. Function $\Lambda(a,b)$, for $a=-0.1910$.

Therefore, we expect that the dynamics generated by the Suris map for fixed δ will resemble, to some extent, those dynamics generated by the two-harmonic mapping given by the Fourier coefficients d_1 and d_2 :

$$\theta' = \theta + r - \frac{2\delta}{\pi} \sin(2\pi\theta) + \frac{\delta^2}{\pi} \sin(4\pi\theta), \tag{11}$$

$$r' = r - \frac{2\delta}{\pi} \sin(2\pi\theta) + \frac{\delta^2}{\pi} \sin(4\pi\theta). \tag{12}$$

We consider the following curve in parameter space:

$$\gamma(\delta) = \left(-\frac{2\delta}{\pi}, \frac{\delta^2}{\pi}\right).$$

As we plot the first roots of the action difference function (8) and the curve described by the coefficients calculated above in the space of parameters, we notice a resemblance

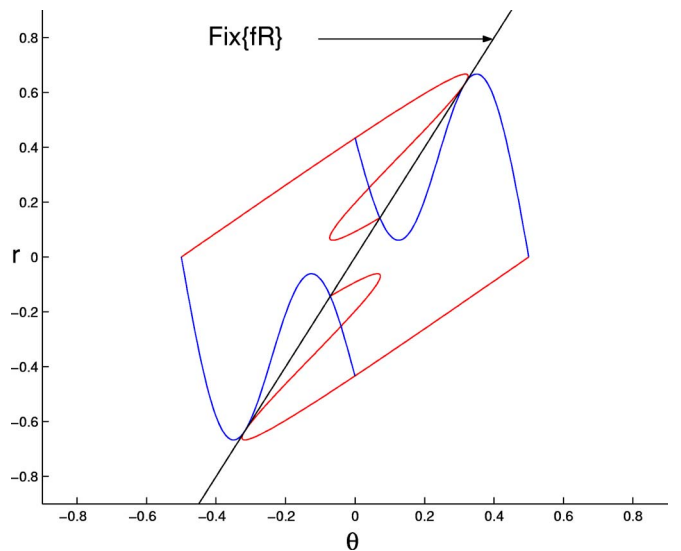


FIG. 12. Stable and unstable manifolds of $p_{1,2}=(\pm 1/2, 0)$, $a^{\dagger}=-0.1910$ and $b^{\dagger}=0.401$.

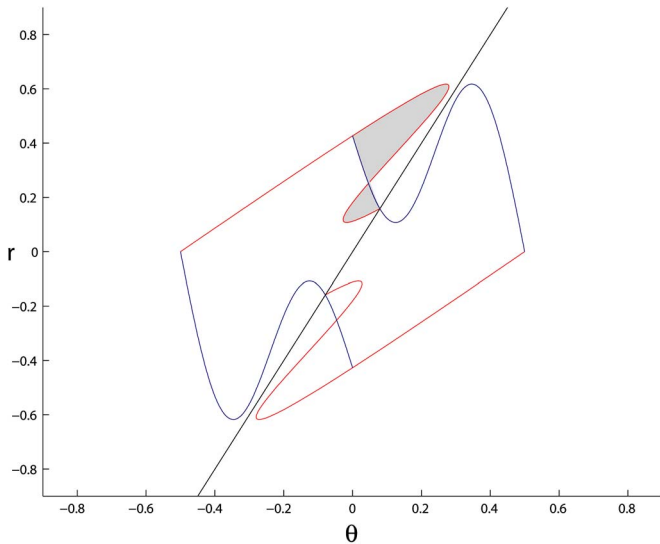


FIG. 13. Stable and unstable manifolds of $p_{1,2}=(\pm 1/2, 0)$, $a=-0.1910$, and $b=0.35$.

between these two curves (see Fig. 10). On the other hand, the curve defined by the second roots withdraws quickly from $\gamma(\delta)$ as b increases.

IV. HETEROCLINIC TANGENCIES

If we look at the graph of the function $\Lambda(a,b)$ for $a=-0.1910$ (see Fig. 11), we discover a discontinuity near $b=0.4$. In Fig. 12, we show the invariant manifolds for parameters where there is a discontinuity in the action difference function. For the value of the discontinuity, the stable and unstable manifolds of two different hyperbolic fixed points intersect tangentially.

Having a tangent intersection of the stable and unstable manifolds has important consequences in global bifurcation theory because this situation is as close to transverseness in

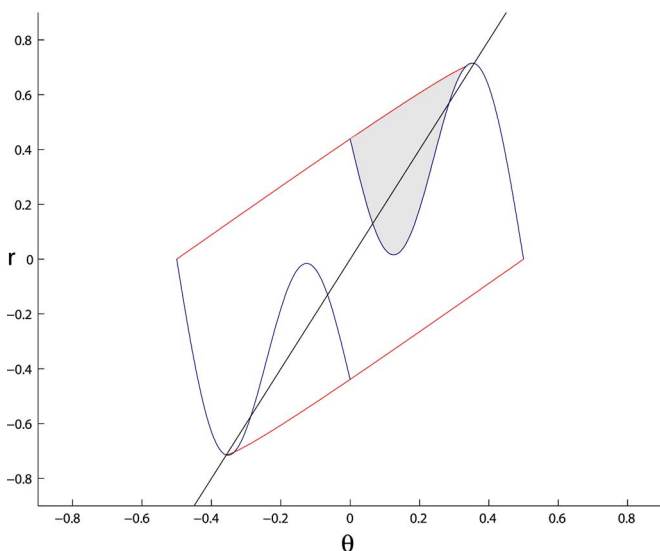


FIG. 14. Stable and unstable manifolds of $p_{1,2}=(\pm 1/2, 0)$, $a=-0.1910$, and $b=0.45$.

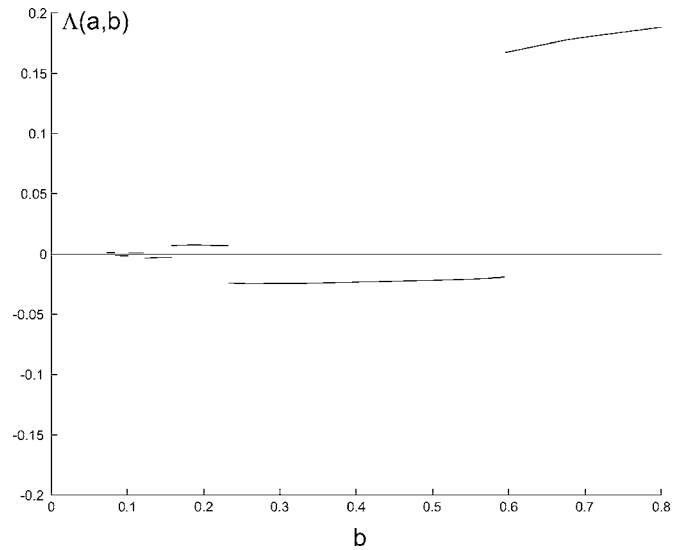


FIG. 15. Function $\Lambda(a,b)$ for $a=-0.0001$.

distance as it is far in essence. Small perturbations applied to a tangent intersections in opposite directions could lead us to completely different dynamics.

The problem of detecting heteroclinic tangencies has been of interest to many authors. For instance, in Ref. 1, the authors prove that a heteroclinic tangency point can imply the existence of a discontinuous change of the chain recurrent and the non-wandering sets. For a definition of these sets, see Ref. 14.

Any such changes in a recurrent set are called an explosion. It has been observed that many of these explosions appear when there is a homoclinic or heteroclinic tangency between stable and unstable manifolds. For instance, suppose that $f : \mathbb{R}^2 \times \mathbb{R} \rightarrow \mathbb{R}^2$ is a C^1 -smooth one-parameter family of C^2 -diffeomorphisms. Following Ref. 1, we define a chain explosion point (x_0, λ_0) as a point such that x_0 is chain recurrent for f_{λ_0} , but there is a neighborhood N of x_0 such that, on one side of λ_0 (either $\lambda < \lambda_0$ or $\lambda > \lambda_0$) no point in N is

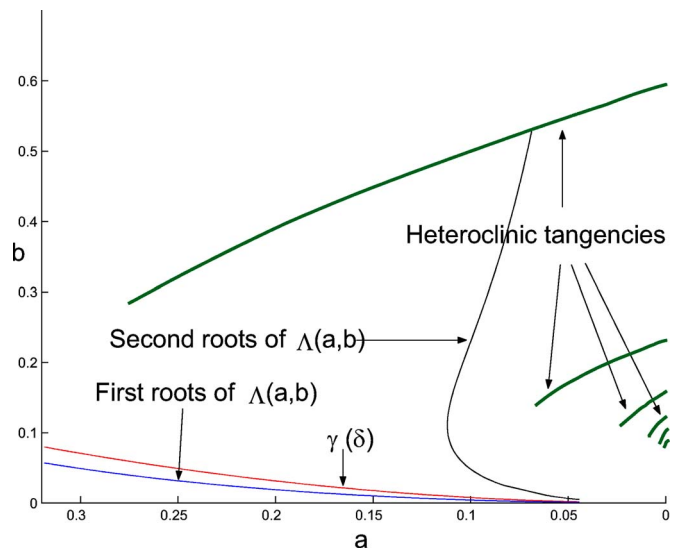


FIG. 16. Two-harmonic map parameter space.

chain recurrent for f_λ . Many chain explosions can be observed when there is a heteroclinic tangency. However, it is not sufficient to have such tangency in order to have a chain explosion. For more information, see Ref. 13.

As we will see, discontinuities of the function Λ are related to the existence of heteroclinic tangencies and sudden changes in the areas of lobes and the rate of transport. The question of whether or not these discontinuities in Λ correspond to some type of explosion is out of the scope of this paper, but could be an interesting extension.

A tangent intersection between the stable and unstable manifolds can produce multilobe phenomena where a perturbation can create new lobes and, by doing so, new turnstiles. Therefore, a perturbation of this kind of intersections may affect, in some way, the transport of the unperturbed system.

In Figs. 13 and 14, we plotted the manifolds for two pairs of parameters close to $(a^\dagger, b^\dagger) = (-0.1910, 0.4)$. Notice that the point of the heteroclinic orbit that lies on the set $\text{Fix}\{Rf\}$ changes drastically in the two figures. For small fixed values of a there are several tangent intersections corresponding to several values of b (see Fig. 15). As in the case shown in Figs. 11–14, if we plot the stable and unstable manifolds in phase space for $a = -0.0001$ and values of b chosen where the graph of Λ has a discontinuity, we would observe the invariant manifolds of $p_{1,2} = (\pm 1/2, 0)$ intersect tangentially. As argued before, in Fig. 15 we expect to detect many heteroclinic tangencies since a is small.

V. CONCLUSION

We have studied invariant manifolds for the two-harmonic standard map. Using the reversor method, we found two different heteroclinic orbits between a pair of saddle points. We defined a function Λ that measures the difference in action between these two orbits. We found that the function Λ can also predict topological bifurcations in the heteroclinic intersections and, in particular, predict the existence of tangential intersections and changes of orientation in

the lobes. One of the bifurcations is explained by the proximity to an integrable map. It would be nice to study if this is a general feature of standard maps.

A summary of first roots, second roots and heteroclinic tangencies can be found in Fig. 16. In this figure, the parameter space is shown and these special points are plotted. In the future, we would like to apply the same methods and study standard maps with different potentials. In addition, we conjecture that there are small-angle phenomena that need to be studied. With this, we would like to verify that the geometric flux quantifies the transport observed numerically.

¹K. Alligood, E. Sander, and J. Yorke, *Ergod. Theory Dyn. Syst.* **22**, 953–972 (2002).

²C. Baesens and R. S. MacKay, *Physica D* **71**, 372–389 (1994).

³L. Faddeev and A. Y. Volkov, *Lett. Math. Phys.* **32**, 125–135 (1994).

⁴C. Golé, *Symplectic Twist Maps*, in *Advanced Series in Nonlinear Dynamics* Vol. 18 (World Scientific, River Edge, NJ, 2001).

⁵V. F. Lazutkin, *Algebra Anal.* **1**, 116–131 (1989).

⁶H. E. Lomelí, *Ergod. Theory Dyn. Syst.* **17**, 445–462 (1997).

⁷H. E. Lomelí and J. D. Meiss, *Phys. Lett. A* **269**, 309–318 (2000).

⁸R. S. MacKay, J. D. Meiss, and I. C. Percival, *Physica D* **13**, 55–81 (1984).

⁹R. S. MacKay, J. D. Meiss, and I. C. Percival, *Physica D* **27**, 1–20 (1987).

¹⁰J. D. Meiss, *Rev. Mod. Phys.* **64**, 795–848 (1992).

¹¹J. Nocedal and S. Wright, *Numerical Optimization*, in *Springer Series in Operations Research* (Springer-Verlag, New York, 2000).

¹²T. Qian and Z. Xia, *Discrete Contin. Dyn. Syst.* **9**, 69–95 (2003).

¹³C. Robert, K. T. Alligood, E. Ott, and J. A. Yorke, *Physica D* **144**, 44–61 (2000).

¹⁴M. Shub, *Global Stability of Dynamical Systems* (Springer-Verlag, New York, 1987).

¹⁵D. Sterling, H. R. Dullin, and J. D. Meiss, *Physica D* **134**, 153–184 (1999).

¹⁶Y. B. Suris, *Funct. Anal. Appl.* **23**, 74–75 (1989).

¹⁷E. Tabacman, *Physica D* **85**, 548–562 (1995).

¹⁸Q. Wang, *Variational Construction of Heteroclinic Orbits for the Monotone Twist Maps*, preprint (Vanderbilt University, Nashville, TN, May 1995).

¹⁹Q. Wang, in *Hamiltonian Dynamics and Celestial Mechanics: A Joint Summer Research Conference on Hamiltonian Dynamics and Celestial Mechanics, June 25–29, 1995, Seattle, Washington*, *Contemp. Math.* Vol. 198 (Amer. Math. Soc., Providence, RI, 1996), pp. 197–206.

²⁰S. Wiggins, *Chaotic Transport in Dynamical Systems*, in *Interdisciplinary Applied Mathematics* Vol. 2 (Springer-Verlag, New York, 1992).

²¹Y. Yamaguchi and K. Tanikawa, *Phys. Lett. A* **280**, 33–36 (2001).